Journal of Hazardous Materials 164 (2009) 301–309

Contents lists available at ScienceDirect

Journal of Hazardous Materials

journal homepage: www.elsevier.com/locate/jhazmat

Interaction of 2,4,6-trichlorophenol with high carbon iron filings: Reaction and sorption mechanisms

Alok Sinha, Purnendu Bose*

Environmental Engineering and Management Programme, Department of Civil Engineering, Indian Institute of Technology Kanpur, Kanpur 208016, India

ARTICLE INFO

Article history:
Received 26 March 2007
Received in revised form 8 July 2008
Accepted 4 August 2008
Available online 13 August 2008

Keywords:
2,4,6-Trichlorophenol
2,4-Dichlorophenol
Reductive dehalogenation
High carbon iron filings (HCIF)

ABSTRACT

Reductive dehalogenation of 2,4,6-trichlorophenol (2,4,6-TCP) by two types of high carbon iron filings (HCIF), HCIF-1 and HCIF-2 was studied in batch reactors. While the iron, copper, manganese and carbon content of the two types of HCIF was similar, the specific surface area of HCIF-1 and HCIF-2 were 1.944 and 3.418 $m^2 g^{-1}$, respectively. During interaction with HCIF-1, 2,4,6-TCP adsorbed on HCIF-1 surface resulting in rapid reduction of aqueous phase 2,4,6-TCP concentration. However, reductive dehalogenation of 2,4,6-TCP was negligible. During interaction between 2,4,6-TCP and HCIF-2, both 2,4,6-TCP adsorption on HCIF-2, and 2,4,6,-TCP dechlorination was observed. 2,4,6-TCP partitioning between solid and aqueous phase could be described by a Freundlich isotherm, while 2,4,6-TCP dechlorination could be described by an appropriate rate expression. A mathematical model was developed for describing the overall interaction of 2,4,6-TCP with HCIF-2, incorporating simultaneous adsorption/desorption and dechlorination reactions of 2,4,6-TCP with the HCIF surface. 2,4-Dichlorophenol (2,4-DCP), 2-chlorophenol (2-CP) and minor amounts of 4-chlorophenol (4-CP) evolved as 2,4,6-TCP dechlorination by-products. The evolved 2,4-DCP partitioned strongly to the HCIF surface. 4-CP and 2-CP accumulated in the aqueous phase. No transformation of 2-CP or 4-CP to phenol was observed.

1. Introduction

Chlorophenols are recalcitrant compounds that are extensively used as biocides, wood preservatives and intermediates to the manufacture of herbicides, pesticides, higher chlorinated congeners and dyes. They are also produced as disinfection by-products during chlorination of wastewater and drinking water and during bleaching of wood pulp with chlorine [1,2]. Most chlorophenols have been listed as priority pollutants by USEPA [3] due to their toxicity and persistence.

Degaradation of chlorophenols have been studied by various chemical methods like ozonation [4], Fenton oxidation [5], photo-peroxidation [6], photo-Fenton process [7], electrochemical oxidation [8], electrochemical reduction [9], sonication [10], catalytic hydrodechlorination [11], photo-electrochemical oxidation [12] and supercritical water oxidation [13]. Biodegradation studies include aerobic [14,15] and anaerobic [16,17] degradation of chlorophenols.

In the last decade, zero-valent metals and bimetallic systems have been used to dechlorinate chlorophenols. The rates of dechlorination are often higher in such systems as compared to biodegradation [18–23]. Kim and Carraway [18] studied dechlorination of pentachlorophenol (PCP) by zero-valent iron (ZVI) and ZVI modified through addition of palladium (Pd), platinum, nickel and copper. Rapid decline in initial concentrations of PCP during this study was attributed to a combination of sorption of PCP to the ZVI surface and dehalogenation reactions. Several tetra-chlorophenol isomers were identified as dechlorination by-products. PCP dechlorination rates with ZVI were reported to be higher than with amended ZVIs. Liu et al. [19] reported dechlorination of *ortho*-, *meta*- and *para*-chlorophenol by Pd impregnated ZVI. Rate of chlorophenol conversion to phenol increased with increase in Pd loading from 0 to 0.1 wt%. Dechlorination of 4-chlorophenol (4-CP), 2,6-dichlorophenol (2,6-DCP), 2,4,6-trichlorophenol (2,4,6-TCP) and PCP by ZVI and zero-valent magnesium (ZVM), with and without added Pd was reported [20]. In 240 min reaction time, PCP was not dehalogenated by ZVI. Slow dehalogenation was observed using Pd-ZVI and ZVM, while rapid dehalogenation was observed when Pd-ZVM was used. Various tetra-chlorophenol isomers, 2,4,6-TCP, phenol, cyclohexanol and cyclohexanone were observed as by-products. 4-CP, 2,6-DCP, and 2,4,6-TCP were

* Corresponding author. Tel.: +91 512 2597403; fax: +91 512 2597395.
E-mail address: pbose@iitk.ac.in (P. Bose).

0304-3894/$ – see front matter © 2008 Published by Elsevier B.V.
doi:10.1016/j.jhazmat.2008.08.005

degraded significantly only by the Pd/ZVM systems. Wei et al. [21] reported dechlorination of *ortho*-chlorophenol by nano-scale ZVI impregnated with Pd. In another related study [22], dechlorination of 2,4-dichlorophenol (2,4-DCP) by nano-scale ZVI impregnated with Pd was reported. 2,4-DCP was completely dehalogenated over a time period of 5 h. 2-Chlorophenol (2-CP), 4-CP and phenol were observed as by-products. Interaction of 2-4-DCP with same mass of micron-sized ZVI resulted in barely 5% conversion over 1 h, suggesting increased surface area and presence of Pd resulted in faster dechlorination by nono-scale ZVI. Dehalogenation of chlorophenols by magnesium–silver bimetallic systems has also been reported [23]. PCP dechlorination was accompanied by the accumulation of tetra-, tri- and dichlorophenols in the system. Dechlorination studies using 2,3,4,6-tetrachlorophenol and 2,4,5-trichlorophenol in a similar system indicated that dechlorination of chlorophenols decreased with the number of chlorine atoms on the target compound.

Based on the review of literature following conclusions can be drawn regarding dechlorination of chlorphenols by ZVI. First, interaction with nano-scale ZVI having large specific surface area will result in faster dechlorination of chlorophenols as compared to interaction with micron sized ZVI. Second, impregnation of ZVI with Pd or other metals may enhance chlorophenol dechlorination rates. Third, removal of the target chlorophenol from the aqueous phase is not a sufficient indication of dehalogenation, since adsorption of chlorophenol on ZVI surface has been observed in many cases. Fourth, chlorophenols with larger number of chlorine atoms are expected to dechlorinate faster.

Due to its low cost [24], micron sized HCIF is the material of choice for use in continuous systems such as permeable reactive barriers (PRBs), which are often employed for degradation of halogenated organic compounds (HOCs) present in contaminated groundwater. 2,4,6-TCP has been listed as a priority pollutant by USEPA [3] due to its toxicity and persistence. During interaction with HCIF, 2,4,6-TCP is expected to undergo reductive dechlorination. Further, 2,4,6-TCP being relatively hydrophobic is expected to partition like other hydrophobic HOCs on graphite inclusions present in the HCIF surface [25,26]. However, adsorption of 2,4,6-TCP is complicated by the fact that it exists in both non-dissociated and dissociated forms, with the relative abundance of the two forms being dependent on solution pH. In case of a surface with charged functional groups, e.g., the activated carbon or metal oxide surface, both non-ionic and ionic forms of 2,4,6-TCP are expected to adsorb on the surface [27]. However in case of adsorption on soil organic carbon, where partitioning is mainly through hydrophobic interactions, the situation may be substantially different. It has been reported that the ionized form of PCP has a lower tendency to partition to soil organic carbon than the non-ionized form [28,29]. Based on similar reasoning, it is expected that adsorption of 2,4,6-TCP on the HCIF surface will be predominantly through the hydrophobic interaction of the of the non-dissociated form of 2,4,6-TCP with the graphite inclusions on the HCIF surface, while the dissociated form will remain predominantly in the aqueous phase.

The objective of the present study was to investigate and understand the interaction of 2,4,6-TCP with HCIF. Specifically the objectives were:

- To study the extent of reductive dehalogenation of 2,4,6-TCP by HCIF.
- To elucidate and model the process of concurrent adsorption and reductive dechlorination of 2,4,6-TCP by HCIF.
- To elucidate pathways of reductive dechlorination of 2,4,6-TCP during interaction with HCIF.

2. Materials and methods

2.1. Materials

Commercially available high carbon iron was chipped on a lathe machine and then ground into iron filings in a ball mill. The filings were between 40 and 80 mesh size. HCIF thus produced was washed in N_2-sparged 1N HCl with periodic shaking for 30 min, then rinsed 10–12 times with N_2-sparged deionized (Milli-Q) water, and dried for 1 h at 100 °C in N_2 atmosphere. This treatment yielded black metallic filings with no visible rust on the surface. X-ray diffraction (XRD) spectra of the pre-treated HCIF surface were obtained using X-ray Powder Diffractometer (Model ISO-Debyeflex 2002, Rich Seifert & Co., Germany) using Cu Kα radiation. XRD results (not shown) indicated that the HCIF surface was devoid of any oxide coating. HCIF was stored in a vacuum desiccator until use in various experiments.

Two batches of HCIF were prepared as above. Surface area of the first (HCIF-1) and second batch (HCIF-2) of HCIF was determined by BET (N_2) analysis using a BET surface area analyzer (Coulter SA 3100, USA) to be 1.944 and 3.418 $m^2\ g^{-1}$, respectively. Carbon content of HCIF-1 and HCIF-2 was determined using the Strohlein Apparatus (Adair Dutt & Co. Pvt. Ltd., India) to be 2.8 and 2.72 wt%. Samples of HCIF-1 and HCIF-2 were digested in aqua-regia and analyzed by atomic absorption spectrometer (AAS) (VARIAN, Spectra AA, 220FS, Australia) for determination of metal content. The iron, copper and manganese content of HCIF-1 was 94.4, 0.1 and 0.375 wt%, respectively, while the respective values for HCIF-2 were 93, 0.05 and 0.3%.

Other chemicals used were 2,4,6-TCP (98%, Sigma–Aldrich), 2,4-DCP (99%, Sigma–Aldrich), 2,6-DCP (>99%, Sigma–Aldrich), 2-CP (>99%, Sigma–Aldrich), 4-CP (>99%, Sigma–Aldrich), phenol (>99%, Sigma–Aldrich), cyclohexanol (99%, Sigma–Aldrich), cyclohexanone (99.8%, Sigma–Aldrich), 1,4-dichlorobenzene (>99%, Sigma–Aldrich), *n*-hexane (Merck HPLC Grade), isopropyl alcohol (Merck, HPLC grade), pyrite (Ward's Natural Science Est., Inc., USA), HCl (AR Grade, Thomas Baker) and HNO_3 (AR Grade, Thomas Baker). All chemicals except pyrite were used as is. The pyrite was ground into a fine powder before use. 1 g of ground pyrite was digested in aqua-regia and analyzed by AAS for iron content. This analysis revealed the purity of pyrite to be 94%.

2.2. Experimental procedure

Batch experiments were carried out in 16 mL glass vials with screw caps equipped with teflon lined rubber septa (Wheaton Science, USA). For a typical experiment, approximately 5 g of HCIF and 0.1 g of pyrite was added to a vial, with the exact weight of HCIF and pyrite added being determined gravimetrically. Pyrite addition was for the purpose of pH control. HCIF-1 was contacted with aqueous solutions of 2,4,6-TCP, and 2,4-DCP. HCIF-2 was contacted with only 2,4,6-TCP. Stock solutions of the above chlorophenols were prepared in 1:1 (v/v) mixture of isopropyl alcohol and deionized water. Aqueous solutions of 2,4,6-TCP and 2,4-DCP were prepared by adding the required volume of the stock solution to N_2 sparged deionized water. This solution was then transferred to a 1 L separatory funnel and was purged with N_2 to maintain anoxic conditions. Vials containing HCIF and pyrite were filled from the funnel such that no headspace existed, and then sealed using the vial screw caps. Aqueous volumes in these vials were determined gravimetrically. Control vials, containing chlorophenols but no HCIF or pyrite, were also prepared.

In experiments involving HCIF-1, approximate concentration of 2,4,6-TCP and 2,4-DCP in a vial was 200 and 250 $\mu mol\ L^{-1}$,

respectively. In experiments involving HCIF-2, approximate concentration of 2,4,6-TCP in a vial was 260 μmol L^{-1}. For each compound–HCIF combination, at least two or more identical vials were prepared. All vials were placed on a roller drum and rotated at 15 rpm such that the vial axis remained horizontal at all times. Ambient temperature was approximately 20 ± 2 °C during mixing. Vials were removed (in duplicate and one control) at specified times for sampling and analysis. Before sampling, pH and redox potential were measured *in situ* in all vials.

2.3. Extraction

Both aqueous and sorbed concentration of chlorophenols was measured in all vials. In experiments involving HCIF-1, duplicate 10 μL aliquots of aqueous phase were sampled from each vial using a micro syringe. Each 10 μL aliquot was added to a GC vial containing 1 mL *n*-hexane as solvent and 1,4-DCB as internal standard along with 2 drops of concentrated HCl [20] and sealed. The mixture was then thoroughly mixed on a vortex mixer to ensure partitioning of chlorophenols to the solvent phase and the solvent analyzed using a gas chromatograph equipped with an electron capture detector (GC-ECD). Preliminary experiments indicated that extraction efficiency for 2,4,6-TCP and 2,4-DCP was 94–100% using this method. For determining solid phase concentration, aqueous content of the 16 mL vial was transferred, as far as practicable, to a pre-weighed and sealed 60 mL vial by air displacement using a cannula. The 60 mL vial was weighed after the transfer for determination of the weight and hence volume of the transferred aqueous phase. Next, 5 mL of *n*-hexane and 2 drops of concentrated HCl was added to the 16 mL vial. Vial contents were vortex mixed for 5 min to ensure transfer of the solid phase chlorophenols to the solvent. This extract was transferred to a 10 mL sealed vial. The procedure was repeated. The combined extract was diluted 50 times and analyzed by GC-ECD. Using this value, along with the aqueous phase concentration measured earlier, and through application of associated corrections to account for (1) chlorophenol mass in the aqueous phase removed from the original 16 mL vial to measure the aqueous phase chlorophenol concentration and (2) chlorophenol mass in aqueous phase which could not be separated from the solid phase, mass of chlorophenol adsorbed on HCIF could be calculated. Comparison of the total added mass of 2,4,6-TCP with the sum of measured aqueous and solid-phase mass of 2,4,6-TCP for the sample after 2 h contact time (amount of 2,4,6-TCP dehalogenation was negligible in 2 h) showed greater than 99% recovery, thus validating the analytical procedure. The same procedure applied to 2,4-DCP resulted in 97% recovery after 2 h contact.

In experiments involving HCIF-2, 1 mL of aqueous solution from the 16 mL vials was transferred to a GC vial containing 0.5 mL of *n*-hexane (with 1,4-DCB as internal standard) along with 2 drops of HCl and sealed. The contents were mixed on a vortex mixer for 5 min to ensure partition of chlorophenols to the solvent phase. To ensure accurate quantification, for some samples, the solvent phase was concentrated by purging with N_2 before analysis. The solvent phase was analyzed by a gas chromatograph equipped with flame ionization detector (GC-FID). Preliminary experiments showed that recoveries using this method were 90–100% for tri- and di-chlorophenols and 70–80% for mono-chlorophenols. To measure the solid phase concentration, 1 mL of 0.1N NaOH solution was added to the 16 mL vial and vortex mixed for 10 min. Addition of NaOH facilitated desorption of sorbed chlorophenols to the aqueous phase [30]. The contents of the vials were sampled as before for determination of total chlorophenols concentration. This method resulted in 90–115% recovery of 2,4,6-TCP and 2,4-DCP after 2 h of contact with HCIF.

2.4. Analytical methods

pH and oxidation–reduction potential (ORP) of the aqueous phase in all vials were measured before sampling of the vials. Needle type microelectrodes were pierced through the septa for these measurements. A redox electrode (Model: MI-800/414, Microelectrodes Inc., USA) and a combination pH electrode (Model: MI-414, Microelectrodes, Inc., USA) connected to an Orion 320 PerpHecT analyzer (Thermo Scientific, USA) was employed for this purpose.

In case of experiments involving HCIF-1, chlorophenols concentration was measured using GC-ECD. A PerkinElmer Clarus 500 gas chromatograph equipped with an Elite-5 column (30 m × 0.32 mm × 0.25 μm) was used for measurement of chlorophenols concentration. Carrier gas was N_2 at a velocity of 30 cm s^{-1}. Injector and detector (ECD) temperature were 240 and 375 °C, respectively. The oven temperature program was as follows: 40–150 °C at a ramp of 4 °C/min and hold for 3 min. Samples (1 μL) were injected in splitless mode. Detection limit was 1 pg/μL for 2,4,6-TCP, 10 pg/μL for 2,4-DCP, 50 pg/μL for 2,6-DCP, and 4 ng/μL for 2-CP and 4-CP.

In case of experiments involving HCIF-2, chlorophenols concentration was measured using GC-FID. A PerkinElmer Clarus 500 gas chromatograph equipped with an Elite-5 column (30 m × 0.53 mm × 0.5 μm) was used for measurement of chlorophenols concentration. Carrier gas was N_2 at a velocity of 17 cm/s. Injector and detector (FID) temperature were 240 and 330 °C, respectively. The oven temperature program was as follows: 70–90 °C at a ramp of 4 °C/min and hold for 1 min, 90–185 °C at a ramp of 15 °C/min and hold for 5 min. Samples (1 μL) were injected in splitless mode. Detection limit was 1 ng/μL for all chlorophenols analyzed.

3. Results and discussion

3.1. Interaction of HCIF-1 with 2,4,6-TCP

Interaction of 2,4,6-TCP with HCIF-1 in 16 mL vials containing 5 g (approximately 323 g L^{-1}) HCIF-1 resulted in decline in 2,4,6-TCP aqueous concentration (C_a, μmol L^{-1}) from 200 to 100 μmol L^{-1} in 60 h (see Fig. 1A), beyond which the 2,4,6-TCP aqueous concentration remained nearly constant over the experimental duration of 800 h. Despite addition of pyrite as a buffering agent, pH was observed to increase from an initial value of 6.5 to approximately 7.2 within 60 h (see Fig. 1B), beyond which pH remained approximately constant. Solid phase 2,4,6-TCP concentration (C_s, μmol g^{-1} iron) also increased to the maximum value within 60 h (see Fig. 1C). Only 2,4,6-TCP dechlorination by-product identified was 2,4-DCP, which remained adsorbed to the solid phase (see Fig. 1C). The measured concentration of 2,4-DCP was less than 1% of the total amount of 2,4,6-TCP added.

2,4,6-TCP exists in aqueous phase in both non-dissociated and dissociated forms, with the fraction in each form being determined by aqueous phase pH and the dissociation constant for 2,4,6-TCP ($K_{TCP} = 10^{-6.4}$). Hence, C_a may be apportioned into the non-dissociated aqueous phase $(C_a)_1$ (μmol L^{-1}) and the dissociated aqueous phase $(C_a)_2$ (μmol L^{-1}) fractions. Also,

$$(C_a)_1 \underset{k_3}{\overset{k_2}{\rightleftarrows}} (C_a)_2 + H^+, \quad K_{TCP} = \frac{k_2}{k_3}, \tag{1}$$

where k_2 (h^{-1}) and k_3 (μmol^{-1} L h^{-1}) are the reaction rate constants for 2,4,6-TCP deprotonation and protonation reactions, respectively, and K_{TCP} (M) is the equilibrium constant. Also,

$$C_a = (C_a)_1 + (C_a)_2 \tag{2}$$

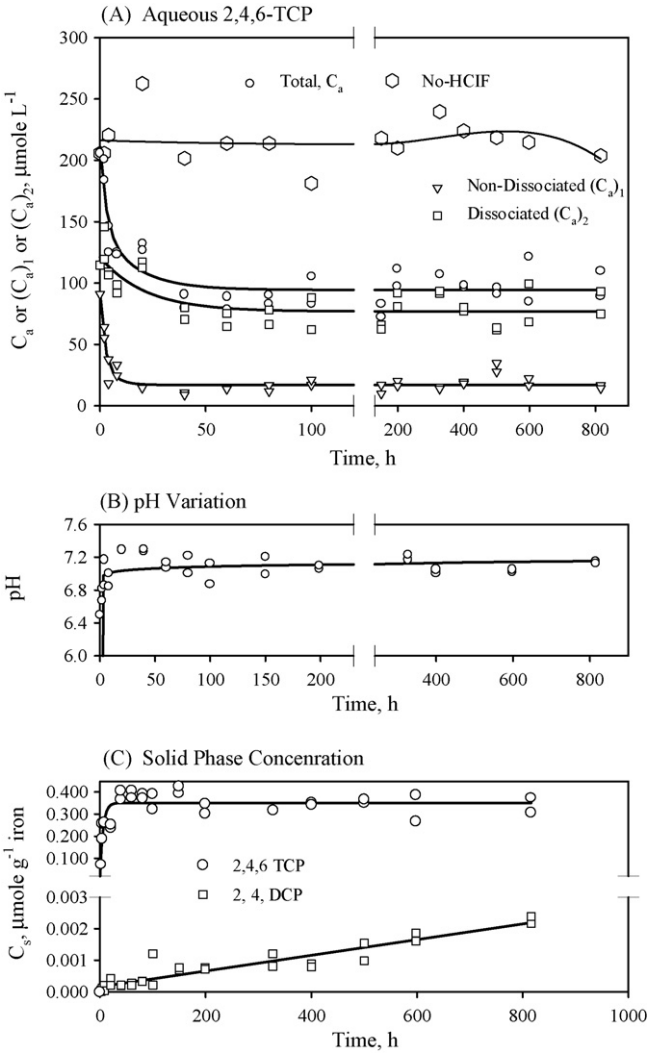

Fig. 1. Interaction of 2,4,6-TCP with HCIF-1 (HCIF-1 concentration: 323 g L^{-1}). (A) Variation of 2,4,6-TCP aqueous concentration with time. (B) Temporal variation of pH in batch reactors. (C) Variation of 2,4,6-TCP sorbed concentration with time and evolution of 2,4-DCP as a by-product of dehalogenation.

$$(C_a)_1 = \frac{[H^+]}{[H^+] + K_{TCP}} C_a \quad (3)$$

$$(C_a)_2 = \frac{K_{TCP}}{[H^+] + K_{TCP}} C_a \quad (4)$$

Total measured aqueous phase 2,4,6-TCP (C_a) as been apportioned using Eqs. (3) and (4), and using pH values presented in Fig. 1B. The resulting $(C_a)_1$ and $(C_a)_2$ concentrations are shown in Fig. 1A.

Preliminary experiments involving the interaction of electrolytic iron (containing no carbon) with 2,4,6-TCP and other chlorophenols showed that chlorophenols do not adsorb on the electrolytic iron surface. Results presented in Fig. 1A and C however suggest that the major interaction between 2,4,6-TCP and HCIF was the adsorption of non-dissociated 2,4,6-TCP as described above. Hence it is logical to conclude that during interaction with HCIF, the observed adsorption is attributable to the presence of carbon in HCIF.

Dechlorination of 2,4,6-TCP by the HCIF surface was of negligible consequence. The basis of this conclusion is two-folds, first, no dechlorination by-products except very low amounts of 2,4-DCP was observed, and second, gradual long-term decline in either

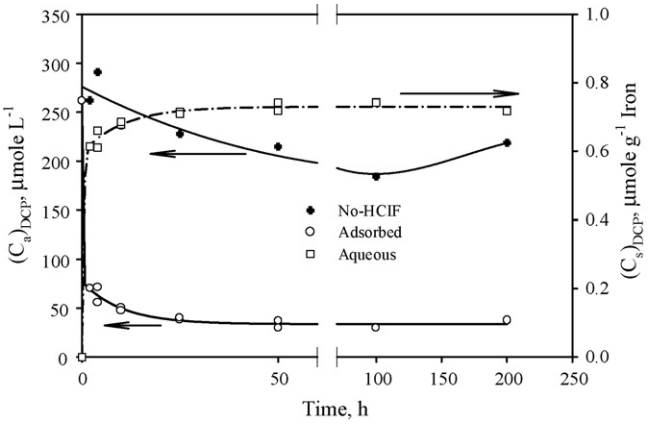

Fig. 2. Temporal variation of aqueous and sorbed concentration of 2,4-DCP during interaction with HCIF-1 (HCIF-1 concentration: 323 g L^{-1}).

aqueous phase (C_a) (see Fig. 1A) or solid phase (C_s) (see Fig. 1C) 2,4,6-TCP concentration was not observed, though such decline should be observed in case dechlorination takes place at a reasonable rate. Consequently, the total 2,4,6-TCP concentration (C_T, µmol L^{-1}), remained nearly constant over the experimental duration.

pH was observed to increase during preliminary experiments conducted with vials containing HCIF but no chlorophenols (data not shown). However, when pyrite was added to such vials, pH was found to remain constant. However, in vials containing both HCIF and chlorophenols, pH was observed to increase despite the presence of pyrite. Hence, it was concluded that the increase of pH was due to the interaction between HCIF and chlorophenols. Increase in pH shown in Fig. 1B may be explained by noting that only the non-dissociated form of 2,4,6-TCP is expected to substantially adsorb on the HCIF surface. In that case, aqueous phase non-dissociated 2,4,6-TCP concentration, $(C_a)_1$, will decline. Thus the equilibrium between non-dissociated and dissociated 2,4,6-TCP in the aqueous phase will be disturbed, and to regain equilibrium, some aqueous phase dissociated 2,4,6-TCP will become non-dissociated. Consumption of protons as above will disturb H^+/OH^- equilibrium, leading to dissociation of H_2O. When new H^+/OH^- equilibrium is achieved, the concentration of OH^- will be higher than before, resulting in the observed increase in pH.

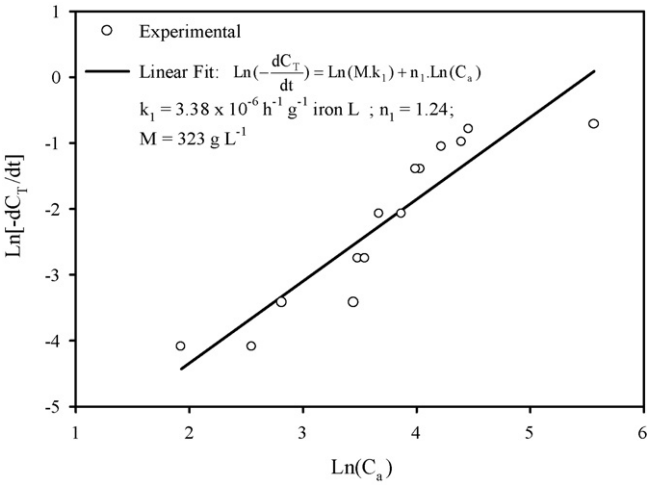

Fig. 3. Interaction of 2,4,6-TCP with HCIF-2 (HCIF-2 concentration: 323 g L^{-1}). (A) Decline in total 2,4,6-TCP concentration with time. (B) Linearized plot of rate of 2,4,6-TCP degradation vs. aqueous phase 2,4,6-TCP concentration.

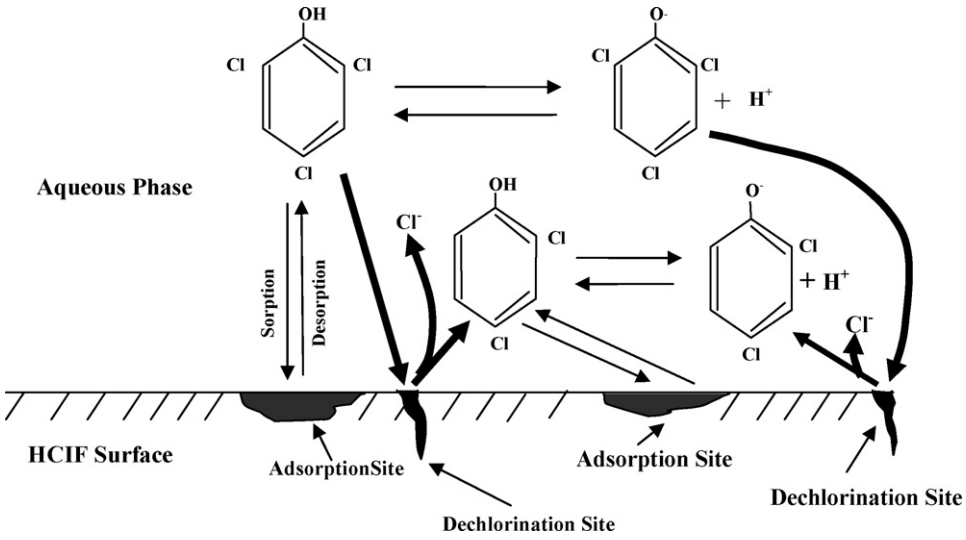

Fig. 4. Schematic of the interaction of 2,4,6-TCP with the HCIF surface.

Interaction between 2,4-DCP and HCIF-1 (see Fig. 2) resulted in initial decline (over first 50 h of interaction) in aqueous 2,4-DCP concentration, $(C_a)_{DCP}$ (μmol L^{-1}), which could be attributed to adsorption of 2,4-DCP on the HCIF surface. No 2,4-DCP dechlorination by-products were observed, while the $(C_a)_{DCP}$ and solid phase 2,4-DCP concentration $(C_s)_{DCP}$ (μmol g^{-1} iron) remained constant beyond the initial 50 h. It was thus concluded that 2,4-DCP was not dechlorinated by HCIF-1 under the experimental conditions investigated.

3.2. Interaction of HCIF-2 with 2,4,6-TCP

Interaction of 2,4,6-TCP with HCIF-2 resulted in an overall decline in the total 2,4,6-TCP concentration (C_T, μmol L^{-1}). The concentration of HCIF-2 (M) was 323 g L^{-1} in these experiments. Decline in C_T was due to dechlorination of 2,4,6-TCP by HCIF. C_T consists of two components, the non-dissociated form $(C_T)_1$ (μmol L^{-1}) and the dissociated form $(C_T)_2$ (μmol L^{-1}). Assuming that rate of dechlorination of both forms of 2,4,6-TCP is identical and dependent on total aqueous 2,4,6-TCP concentration (C_a),

$$n_1 C_a + M \xrightarrow{k_1} \text{Dehalogenation by-products} \quad (5)$$

$$\text{Thus, } \frac{dC_T}{dt} = -k_1 M (C_a)^{n_1} \quad (6)$$

$$\text{Linearizing, } \ln\left(-\frac{dC_T}{dt}\right) = \ln(Mk_1) + n_1 \ln(C_a) \quad (6a)$$

where k_1 (h^{-1} g^{-1} iron L) is the rate and n_1 is the order of the dechlorination reaction, respectively. A plot of $\ln(-dC_T/dt)$ versus $\ln(C_\alpha)$ is shown in Fig. 3. Fitting a linear equation through the data in Fig. 3, values of k_1 and n_1 (see Eq. (6a)) were calculated to be 3.38×10^{-6} h^{-1} g^{-1} iron L and 1.24, respectively.

The overall interaction of 2,4,6-TCP with HCIF-2 is conceptually represented in Fig. 4. Both dechlorination and adsorption reactions are assumed to occur simultaneously. As in case of HCIF-1, it was assumed that only the non-dissociated 2,4,6-TCP partitions to graphite inclusions present in HCIF surface. Partitioning of non-dissociated 2,4,6-TCP to the HCIF surface was assumed to be non-specific in nature, i.e., the number of adsorption sites on the graphite inclusions is constrained only by the number of non-dissociated 2,4,6-TCP molecules that can be fitted on the carbon surface. At low surface coverage, such partitioning can be

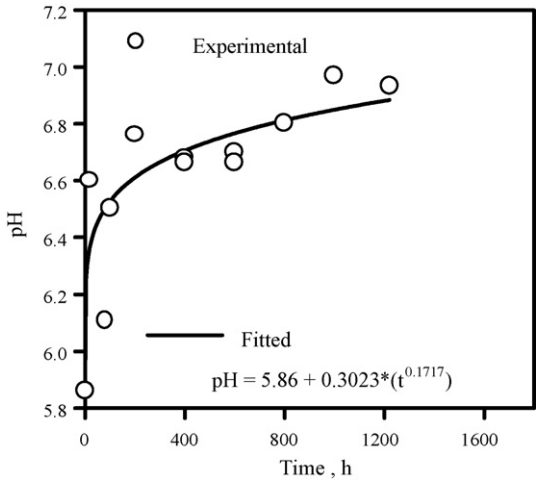

Fig. 5. Variation of pH in batch reactor during interaction of 2,4,6-TCP with HCIF-2 (HCIF-1 concentration: 323 g L^{-1}).

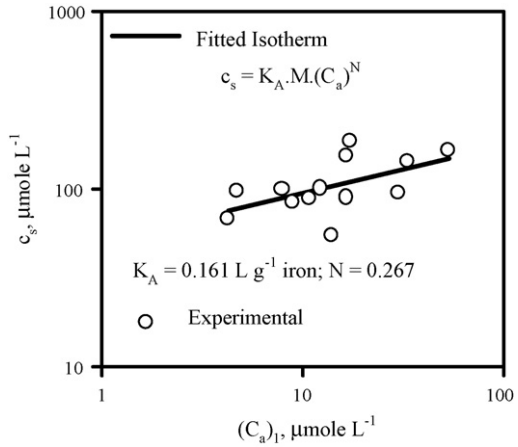

Fig. 6. Plot of non-dissociated aqueous vs. corresponding sorbed concentration of 2,4,6-TCP during interaction with HCIF-2 (HCIF-1 concentration: 323 g L^{-1}).

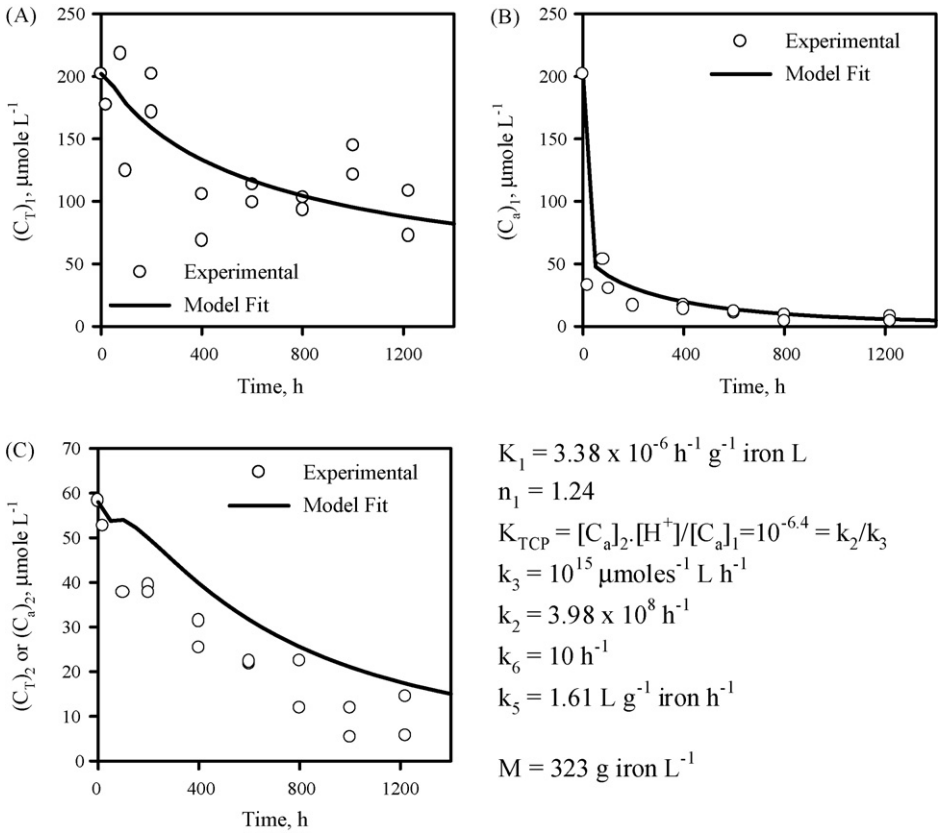

Fig. 7. Simulation of interaction of 2,4,6-TCP with HCIF-2 (HCIF-1 concentration: 323 g L^{-1}). (A) Variation of total non-dissociated concentration of 2,4,6-TCP with time. (B) Variation of aqueous non-dissociated concentration of 2,4,6-TCP with time. (C) Variation of total/aqueous dissociated concentration of 2,4,6-TCP with time.

represented by the general equation,

$$N(C_a)_1 + M \underset{k_6}{\overset{k_5}{\rightleftarrows}} c_s \tag{7a}$$

where k_5 (L g^{-1} iron h^{-1}) and k_6 (h^{-1}) are the adsorption and desorption rate constants, respectively. Also, $c_s = MC_s$, where C_s is the sorbed 2,4,6-TCA concentration expressed in µmol L^{-1}. Assuming the rate of 2,4,6-TCP partitioning is fast in comparison to dechlorination reactions, adsorption equilibrium was assumed to be maintained at all times greater than 50 h after reaction commencement. The corresponding equilibrium constant describing 2,4,6-TCP partitioning is $K_A = k_5/k_6$. Under such conditions, partitioning of 2,4,6-TCP between solid and aqueous phases can be represented by a Freundlich isotherm,

$$c_s = K_A M(C_{a_1})^N \tag{7b}$$

where K_A (L g^{-1} iron) and N are the Freundlich isotherm constants. As in case of the experiment using HCIF-1 described earlier, experimentally obtained C_a values at various times were divided into $(C_a)_1$ and $(C_a)_2$ using Eqs. (3) and (4) and pH variation which occurred over the experimental duration, as shown in Fig. 5. The reason pH increase seen in Fig. 5 was the same as that described during the experiment involving HCIF-1. A plot of $(C_\alpha)_1$ versus C_s and the corresponding linear fit (see Eq. (7b)) is presented in Fig. 6. The data could be adequately represented by the Freundlich isotherm, with $N = 0.267$ and $K_A = 0.161$ (µmol g^{-1} iron)/(µmol L^{-1}).

In addition to Eqs. (1)–(7), following relationships also hold at all times during 2,4,6-TCP interaction with HCIF-2,

$$C_T = (C_T)_1 + (C_T)_2 \tag{8}$$

$$(C_T)_2 = (C_a)_2 \tag{9}$$

$$(C_T)_1 = (C_a)_1 + c_s \tag{10}$$

Variation of $(C_T)_1$, $(C_T)_2$, $(C_a)_1$ and C_s with time during 2,4,6-TCP interaction with HCIF-2 can be represented by the equations below,

$$\frac{d(C_T)_1}{dt} = -\{k_1 M(C_a)_1^{n_1}\} - \{k_2(C_a)_1\} + \{k_3(C_a)_2[H^+]\} \tag{11}$$

$$\frac{d(C_T)_2}{dt} = -\{k_1 M(C_a)_2^{n_1}\} - \{k_3 C_{a_2}[H^+]\} + \{k_2(C_a)_1\} \tag{12}$$

$$\frac{d(C_a)_1}{dt} = -\{k_1 M(C_a)_1\} - \{k_2(C_a)_1\} + \{k_3(C_a)_2[H^+]\} - \{k_5 M(C_a)_1^N\} + \{k_6 C_s\} \tag{13}$$

$$\frac{dC_s}{dt} = \{k_5 M(C_a)_1^N\} - \{k_6 C_s\} \tag{14}$$

Eqs. (11)–(14) were solved simultaneously using PDESOL, a differential equation solver. Following initial conditions were used, at time $t = 0$, $C_s = 0$, $(C_a) = (C_T)_1 = 200$ µmol L^{-1} and $(C_T)_2 = 60$ µmol L^{-1}. Other values used were as follows, $k_1 = 3.38 \times 10^{-6}$ h^{-1} g^{-1} iron L, $n_1 = 1.24$, $M = 323$ g iron L^{-1}. Though k_2 and k_3 were unknown, their ratio K_{TCP} is known. It is also known that rates of deprotonation (k_2) and protonation (k_3) of 2,4,6-TCP are fast compared to 2,4,6-TCP dehalogenation or adsorption–desorption reactions. Thus the protonation rate constant (k_3) was assigned an arbitrarily high value of 10^{15} µmol^{-1} L h^{-1}. Since K_{TCP} is known, corresponding value of the deprotonation rate constant (k_2) was calculated as 3.98×10^8 h^{-1}.

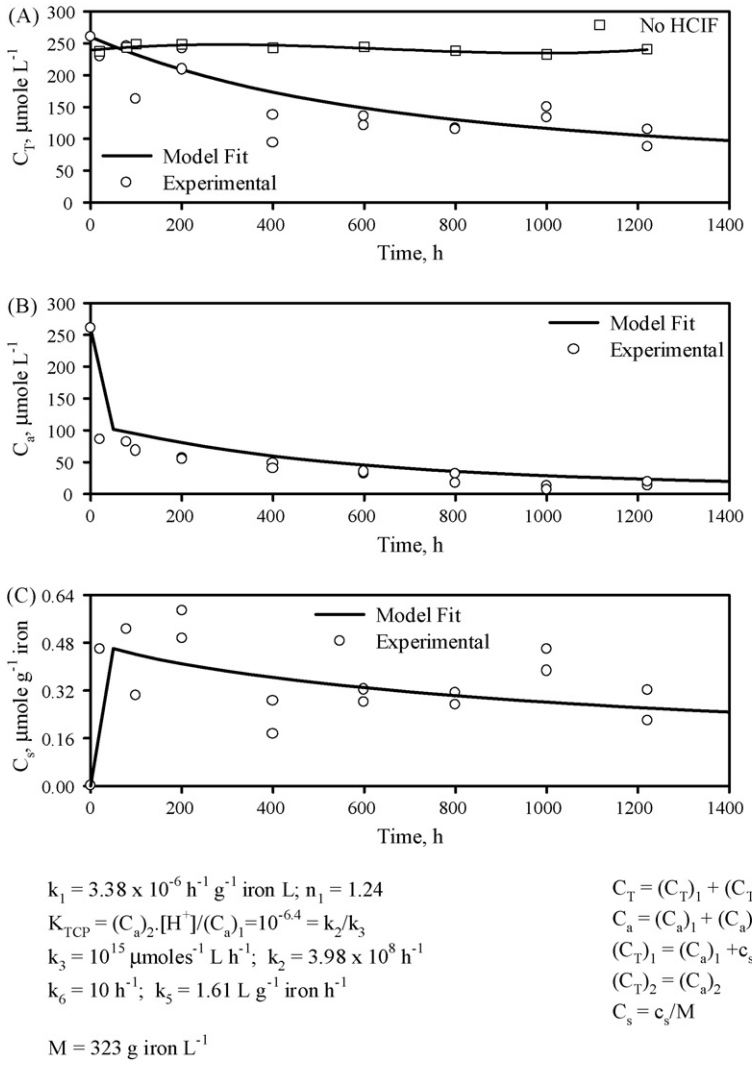

Fig. 8. Simulation of interaction of 2,4,6-TCP with HCIF-2 (HCIF-1 concentration: 323 g L^{-1}). (A) Variation of total concentration of 2,4,6-TCP with time. (B) Variation of aqueous concentration of 2,4,6-TCP with time. (C) Variation of sorbed concentration of 2,4,6-TCP with time.

This ensured the $(C_a)_1$ and $(C_a)_2$ will always remain in equilibrium. The hydrogen ion $[H^+]$ concentration was expressed as a function of time by fitting a curve through the pH data in Fig. 5,

$$pH = 5.86 + 0.3023(t^{0.1717}) \quad (15)$$

This equation was used to obtain $[H^+]$ values required at various times during the solution of Eqs. (11)–(14). The adsorption (k_5) and desorption (k_6) rate constants are also unknown, but their ratio K_A is known. The desorption rate constant (k_6) was used as the fitting parameter to obtain a match between the experimental data and model simulation results. Putting $k_6 = 10\,h^{-1}$, and knowing K_A, k_5 was calculated as 1.61 L g^{-1} iron h^{-1}. Ionic strength effects were not considered. Model simulation with these values fitted the experimental data quite well for $(C_T)_1$ (Fig. 7A) and $(C_a)_1$ (Fig. 7B), but is seen to slightly over-predict $(C_a)_2$ (Fig. 7C). It thus appears that the assumption that dehalogenation rates of non-dissociated and dissociated forms of 2,4,6-TCP being identical was not entirely correct, and dehalogenation rate of dissociated 2,4,6-TCP is probably slightly higher than that of non-dissociated 2,4,6-TCP.

Considering the overall picture, experimental data obtained during interaction of 2,4,6-TCP with HCIF-2 showed an overall decline in total 2,4,6-TCP (C_T) (Fig. 8A), a rapid decrease in the total aqueous 2,4,6-TCP (C_a) followed by a slow decline (Fig. 8B), and a rapid increase in solid phase 2,4,6-TCP (C_s) followed by a slow decline (Fig. 8C). The model simulations results shown in Fig. 8 agree with the experimental results quite closely. The initial rapid decline in C_a and the corresponding rapid increase in C_s was primarily attributed to adsorption of non-dissociated 2,4,6-TCP to the HCIF-2 surface, while slow long-term decline in C_a and C_s was primarily due to dechlorination of 2,4,6-TCP by HCIF-2.

3.3. Discussion

Interaction of 2,4,6-TCP with HCIF-1 resulted in slower dehalogenation as compared to similar interaction with HCIF-2. Iron, copper, manganese and carbon content of both HCIF were similar. Surface characteristics of both HCIF were studied by X-ray diffraction spectrometry. These results were nearly identical, and consistent with that expected for un-rusted iron surface (data not shown). However, the surface area of HCIF-1 and HCIF-2 were determined to be 0.944 and 3.418 $m^2\,g^{-1}$, respectively. Hence it was concluded that the difference in the rates of dehalogenation of 2,4,6-TCP was attributable to the difference in specific surface area between the two batches of HCIF. Considering that the dehalogenation of 2,4,6-TCP occurs through the interaction with the HCIF surface, it is logical to conclude that, with all other things

remaining the same, the HCIF with greater specific surface area would facilitate faster dehalogenation of 2,4,6-TCP. Dechlorination rate of 2-chloronaphthalene by HCIF-1 and HCIF-2 was determined in connection with a related research project, and in that case also, dechlorination rate of 2-chloronaphthalene using HCIF-2 was observed to be much faster as compared to HCIF-1 [26,33].

Reductive dehalogenation of 2,4,6-TCP yielded 2,4-DCP as the primary by-product. 2,4-DCP is expected to be present in non-dissociated state under the prevailing experimental conditions, and hence was adsorbed strongly to the HCIF surface. No 2,6-DCP was identified as a by-product. This showed that the reductive dehalogenation of 2,4,6-TCP occurred through the removal of the chlorine at the *ortho*-position. In contrast, during dechlorination of polychlorinated biphenyls by metallic iron, chlorine at the *para*-position has been observed to be removed [31]. Recently Oh et al. [32] have shown that dechlorination of 2,4-dinitrotoluene in the presence of graphite occurred through the removal of the chlorine at the *ortho*-position, while in the absence of graphite, removal of the chlorine at the *para*-position occurred first. During interaction with HCIF-2 in this study, 2-CP and minor amounts of 4-CP were observed as by-products of 2,4,6-TCP dechlorination (data not shown). This suggested that 2,4-DCP formed as the initial by-product of 2,4,6-TCP dechlorination was further dechlorinated to mainly yield 2-CP. In a recent study involving reduction of 2,4-DCP with nanoscale Pd/Fe it has been shown that the rates of conversion of 2,4-DCP to 2-CP were 2 times faster as compared to conversion to 4-CP [22]. In present study 2-CP seemed to accumulate in aqueous phase and did not transform to phenol as observed by Wei et al. [22] or Liu et al. [19] in a studies involving nano-scale Fe/Pd systems.

4. Summary and conclusions

The interaction of chlorophenols with two types of HCIFs, HCIF-1 and HCIF-2, was studied in batch reactors. Interaction between HCIF-1 and 2,4,6-TCP or 2,4-DCP and between HCIF-2 and 2,4,6-TCP resulted in rapid decline in the aqueous concentration of the target compounds due to partitioning of these compounds to the graphite inclusions present on the surface of HCIF-1 surface. Such rapid decline in aqueous concentration due to sorption can often be mistaken for loss through dechlorination. 2,4,6-TCP was dechlorinated by both HCIF-1 and HCIF-2, with the dechlorination rate being higher with HCIF-2. Major conclusions of this study were:

- Non-dissociated fraction of 2,4,6-TCP was substantially adsorbed to the graphite inclusions present on the surface of HCIF-1 and HCIF-2.
- During interaction with HCIF-2, equilibrium partitioning of the non-dissociated fraction of 2,4,6-TCP between solid and aqueous phase could be described by the Freundlich isotherm, $C_s = K_A M(C_{a1})^N$, with $N = 0.267$ and $K_A = 0.161$ $(\mu mol\, g^{-1}\, iron)/(\mu mol\, L^{-1})$.
- Both non-dissociated and dissociated fractions of 2,4,6-TCP was dechlorinated during interaction with HCIF-2.
- Assuming dechlorination rates of both non-dissociated and dissociated 2,4,6-TCP by HCIF-2 to be identical, this rate could be represented by the expression, $dC_T/dt = -k_1 M(C_a)^{n_1}$, where k_1 and n_1 were $3.38 \times 10^{-6}\, h^{-1}\, g^{-1}$ iron L and 1.24, respectively.
- The simultaneous adsorption/desorption and dechlorination of 2,4,6-TCP by HCIF-2 could be modeled and the model simulation results agree with experimental data quite well.
- 2,4-DCP emerged as the initial by-product of 2,4,6-TCP dechlorination, and remained predominantly sorbed to graphite inclusions present on the HCIF surface. 2,4-DCP produced during experiments involving HCIF-1 did not dechlorinate further.
- 2,4-DCP produced during experiments involving HCIF-2 dechlorinated slowly to 2-CP and minor amounts of 4-CP. These compounds accumulated in the aqueous phase.

Finally, results of this study demonstrate that reductive dechlorination rates of 2,4,6-TCP by HCIF were slow. For HCIF samples of similar composition, rate of reductive dechlorination increased with increase in specific surface area of HCIF. Using HCIF samples with larger specific surface area or modification of HCIF surface through addition of metallic Pd may enhance 2,4,6-TCP dechlorination rates.

References

[1] Agency for Toxic Substances and Disease Registry (ATSDR), Toxicological Profile for Chlorophenols, U.S. Dept. of Health and Human Services, Public Health Service, Atlanta, GA, 1999.
[2] L.J. Graham, J.E. Atwater, G.N. Jovanovic, Chlorophenol dehalogenation in a magnetically stabilized fluidized bed reactor, AICHE J. 52 (2006) 1083–1093.
[3] US Environmental Protection Agency, National Pollutant Discharge Elimination System, Code of Federal Regulations, 40, Part 122, US Government Printing Office, Washington, DC, 1988.
[4] N. Graham, W. Chu, C. Lau, Observations of 2,4,6-trichlorophenol degradation by ozone, Chemosphere 51 (2003) 237–243.
[5] W. Chu, C.K. Law, Treatment of trichlorophenol by catalytic oxidation process, Water Res. 37 (2003) 2339–2346.
[6] W.J. Hou, S. Tsuneda, A. Hirata, TOC removal of 2,4,5-trichlorophenol synthetic wastewater with H_2O_2/UV in a batch reactor, J. Chem. Eng. Jpn. 34 (2001) 1049–1051.
[7] R.F.P. Nogueira, A.G. Trovo, D.F. Mode, Solar photodegradation of dichloroacetic acid and 2,4-dichlorophenol using an enhanced photo-Fenton process, Chemosphere 48 (2002) 385–391.
[8] M.S. Ureta-Zanartu, P. Bustos, C. Berrios, M.C. Diez, M.L. Mora, C. Gutierrez, Electrooxidation of 2,4-dichlorophenol and other polychlorinated phenols at a glassy carbon electrode, Electrochim. Acta 47 (2002) 2399–2406.
[9] H. Cheng, K. Scott, P.A. Christensen, Electrochemical hydrodehalogenation of chlorinated phenols in aqueous solutions. I. Material Aspects, J. Electrochem. Soc. 150 (2003) D17–D24.
[10] Y. Dai, F. Li, F. Ge, F. Zhu, L. Wu, X. Yang, Mechanism of the enhanced degradation of pentachlorophenol by ultrasound in the presence of elemental iron, J. Hazard. Mater. B137 (2006) 1424–1429.
[11] H.M. Roy, C.M. Wai, T. Yuan, J.-K. Kim, W.D. Marshall, Catalytic hyrodechlorination of chlorophenols in aqueous solution under mild conditions, Appl. Catal. A: Gen. 271 (2004) 137–143.
[12] G. Waldner, M. Pourmodjib, R. Bauer, M. Neumann-Spallart, Photoelectrocatalytic degradation of 4-chlorophenol and oxalic acid on titanium dioxide electrodes, Chemosphere 50 (2003) 989–998.
[13] G.H. Lee, T. Nunoura, Y. Matsumura, K. Yamamoto, Effects of sodium hydroxide addition on the decomposition of 2-chlorophenol in supercritical water, Ind. Eng. Chem. Res. 41 (2002) 5427–5431.
[14] S.K. Banerji, R.K. Bajpai, Cometabolism of pentachlorophenol by microbial species, J. Hazard. Mater. 39 (1994) 19–31.
[15] C.M. Kao, C.T. Chai, J.K. Liu, T.Y. Yeh, K.F. Chen, S.C. Chen, Evaluation of natural and enhanced PCP biodegradation at a former pesticide manufacturing plant, Water Res. 38 (2004) 663–672.
[16] B.-V. Chang, C.-W. Chiang, S.-Y. Yuan, Dechlorination of pentachlorophenol in anaerobic sewage sludge, Chemosphere 36 (1998) 537–545.
[17] D.-S. Shen, X.-W. Liu, H.-J. Feng, Effect of easily degradable substrate on anaerobic degradation of pentachlorophenol in an upflow anaerobic sludge blanket (UASB) reactor, J. Hazard. Mater. B119 (2005) 239–243.
[18] Y.-H. Kim, E.R. Carraway, Dechlorination of pentachlorophenol by zero-valent iron and modified zero-valent irons, Environ. Sci. Technol. 34 (2000) 2014–2017.
[19] Y.H. Liu, F.L. Yang, P.L. Yue, G.H. Chen, Catalytic dechlorination of chlorophenols in water by palladium/iron, Water Res. 35 (2001) 1887–1890.
[20] J. Morales, R. Hutcheson, I.F. Cheng, Dechlorination of chlorinated phenols by catalyzed and uncatalyzed Fe(0) and Mg(0) particles, J. Hazard. Mater. B90 (2002) 97–108.
[21] J.J. Wei, X.H. Xu, D.H. Wang, Catalytic dechlorination of *o*-chlorophenol by nanoscale Pd/Fe, J. Environ. Sci. China 16 (2004) 621–623.
[22] J. Wei, X. Xu, Y. Liu, D. Wang, Catalytic hydrodechlorination of 2,4-dichlorophenol over nanoscale Pd/Fe: reaction pathway and some experimental parameters, Water Res. 40 (2006) 348–354.
[23] U. Patel, S. Suresh, Dechlorination of chlorophenols by magnesium–silver bimetallic system, J. Colloid Interface Sci. 299 (2006) 249–259.
[24] D.R. Burris, T.J. Campbell, V.S. Manoranjan, Sorption of trichloroethylene and tetrachloroethylene in a batch reactive metallic iron–water system, Environ. Sci. Technol. 29 (1995) 2850–2855.
[25] D.R. Burris, R.M. Allen-King, V.S. Manoranjan, T.J. Campbell, G.A. Loraine, B. Deng, Chlorinated ethene reduction by cast iron: sorption and mass transfer, J. Environ. Eng. 124 (1998) 1012–1019.

[26] A. Sinha, P. Bose, Dehalogenation of 2-chloronapthalene by cast iron, Water Air Soil Pollut. 172 (2006) 375–390.
[27] P.-O. Nelson, M. Yang, Equilibrium adsorption of chlorophenols on granular activated carbon, Water Environ. Res. 67 (1995) 892–898.
[28] S.-C. Tam, S.A. Johnson, A. Graham, The effect of organic structures on pentachlorophenol adsorption on soil, Water Air Soil Pollut. 115 (1999) 337–346.
[29] M. Cea, J.C. Seaman, A.A. Jara, M.L. Morac, M.C. Diez, Describing chlorophenol sorption on variable-charge soil using the triple-layer model, J. Colloid Interface Sci. 292 (2005) 171–178.
[30] C.N. You, Desorptive behavior of chlorophenols in contaminated soils, Water Sci. Technol. 33 (1996) 263–270.
[31] H.K. Yak, Q. Lang, C.M. Wai, Relative resistance of positional isomers of polychlorinated biphenyls towards reductive dechlorination by zero-valent iron in subcritical water, Environ. Sci. Technol. 34 (2000) 2792–2798.
[32] S. Oh, D.K. Cha, P.C. Chiu, Graphite-mediated reduction of 2,4-dinitrotoluene with elemental iron, Environ. Sci. Technol. 36 (2002) 2178–2184.
[33] A. Sinha, P. Bose, Reactive transport of 2-chloronaphthalene through cast iron filings, in: Proceedings of International Conference on Civil Engineering in the New Millenium: Opportunities and Challenges (CENeM-2007), Bengal Engineering and Science University, WB, India, January 11–14, 2007.